Published in final edited form as:
Am J Physiol Lung Cell Mol Physiol. 2008 June ; 294(6): L1260–L1268. doi:10.1152/ajplung.00035.2008.

Proteasome inhibition improves diaphragm function in congestive heart failure rats

Hieronymus W. H. van Hees[1,3], **Yi-Ping Li**[4], **Coen A. C. Ottenheijm**[1,3,5], **Bingwen Jin**[4], **Cindy J. C. Pigmans**[1], **Marianne Linkels**[1], **P. N. Richard Dekhuijzen**[1,3], and **Leo M. A. Heunks**[1,2,3]

[1] Department of Pulmonary Diseases, Radboud University Nijmegen Medical Centre, Nijmegen, The Netherlands [2] Department of Intensive Care Medicine, Radboud University Nijmegen Medical Centre, Nijmegen, The Netherlands [3] Institute for Fundamental and Clinical Human Movement Sciences, Radboud University Nijmegen Medical Centre, Nijmegen, The Netherlands [4] Department of Medicine, Baylor College of Medicine, Houston, Texas [5] Department of Molecular and Cellular Biology, University of Arizona, Tucson, Arizona

Abstract

In congestive heart failure (CHF), diaphragm weakness is known to occur and is associated with myosin loss and activation of the ubiquitin-proteasome pathway. The effect of modulating proteasome activity on myosin loss and diaphragm function is unknown. The present study investigated the effect of in vivo proteasome inhibition on myosin loss and diaphragm function in CHF rats. Coronary artery ligation was used as an animal model for CHF. Sham-operated rats served as controls. Animals were treated with the proteasome inhibitor bortezomib (intravenously) or received saline (0.9%) injections. Force generating capacity, cross-bridge cycling kinetics, and myosin content were measured in diaphragm single fibers. Proteasome activity, caspase-3 activity, and MuRF-1 and MAFbx mRNA levels were determined in diaphragm homogenates. Proteasome activities in the diaphragm were significantly reduced by bortezomib. Bortezomib treatment significantly improved diaphragm single fiber force generating capacity (~30–40%) and cross-bridge cycling kinetics (~20%) in CHF. Myosin content was ~30% higher in diaphragm fibers from bortezomib-treated CHF rats than saline. Caspase-3 activity was decreased in diaphragm homogenates from bortezomib-treated rats. CHF increased MuRF-1 and MAFbx mRNA expression in the diaphragm, and bortezomib treatment diminished this rise. The present study demonstrates that treatment with a clinically used proteasome inhibitor improves diaphragm function by restoring myosin content in CHF.

Keywords

myosin; bortezomib; single fiber contractility; myosin

The diaphragm is the main inspiratory muscle. Weakness of the diaphragm is associated with dyspnea and increased morbidity and mortality in patients with congestive heart failure (CHF) (21, 29, 31). Although mechanisms of impaired respiratory muscle function are incompletely understood, recent work from our group points toward a prominent role for enhanced myosin degradation through the ubiquitin-proteasome pathway (33, 34, 52). This is of interest as muscle strength strongly depends on myosin content (7, 17). In CHF rats,

Address for reprint requests and other correspondence: H. W. van Hees, Dept. of Pulmonary Diseases-454, Univ. Medical Centre Nijmegen, PO Box 9101, 6500 HB Nijmegen, The Netherlands (H.vanhees@long.umcn.nl).

single fibers dissected from the diaphragm generate less force compared with diaphragm fibers of sham-operated rats (52). Reduction in force generating capacity was proportional to the reduction in myosin content in these fibers. Furthermore, diaphragm weakness in CHF was associated with increased activity of the proteasome. Although these data indirectly suggest that activation of the ubiquitin-proteasome pathway plays a key role in respiratory muscle dysfunction, this was not specifically investigated in previous studies.

Bortezomib is the first proteasome inhibitor that has been approved for use in humans, to treat patients with multiple myeloma (40), and its use in other malignancies is under investigation. Bortezomib is one of the most specific and potent proteasome inhibitors currently available (3, 22) and exhibits relatively mild toxicity (40). Treatment with bortezomib has been shown to prevent muscle mass loss in several experimental conditions (4, 23, 24). However, these studies did not investigate the effect of proteasome inhibition on content of specific contractile proteins, and, more importantly, on muscle function.

The aim of the present study was to investigate the effects of proteasome inhibition on diaphragm function and myosin content in CHF rats. We hypothesized that proteasome inhibition improves diaphragm function by restoring sarcomeric myosin content.

Essential steps in muscle protein degradation act upstream of the proteasome and include ubiquitin-conjugation by specific E3-ligases (6, 47) and caspase-3 activation (13). To further evaluate the mechanisms of contractile protein degradation, we examined the effect of bortezomib on these steps.

METHODS

CHF animal model

Myocardial infarction was induced by ligation of the left coronary artery, as described previously (11, 37, 52). Briefly, adult male Wistar rats (250–300 g) were anesthetized by inhalation of an isoflurane-oxygen mixture (2–5% isoflurane), intubated, and mechanically ventilated. After a left lateral thoracotomy between the fourth and fifth rib, the left coronary artery was ligated at its origin by a 5-0 silk suture. Sham-operated rats underwent a similar procedure without the actual ligation. After the operation and during the following 2 days, buprenorphine (20 μg/kg, subcutaneously) was administered daily for postoperative analgesia.

At the end of the experiment, rats were anesthetized with pentobarbital (70 mg/kg ip) and mechanically ventilated. Aortic pressure and left ventricular pressures were measured by a micromanometer-tipped catheter (SPC 330, Millar Instruments) inserted through the right carotid artery. After a combined thoracotomy/laparotomy, the diaphragm muscle and adherent ribs were quickly excised and divided in parts. One part was snap-frozen in liquid nitrogen and stored at −80°C for later biochemical analyses, and the other parts were prepared for contractile measurements. As described previously, heart weight and infarct size were determined, and lung wet-to-dry ratio was assessed (52). Only data from rats with infarcts >35% of the left ventricle (n = 25) were analyzed. This study was approved by the Animal Ethics Committee, Radboud University Nijmegen, The Netherlands. During the experiments, animals were fed ad libitum.

Treatment with proteasome inhibitor

Thirteen weeks after coronary artery ligation (n = 25) or sham operation (n = 17), animals were randomly assigned to bortezomib treatment or control group. Bortezomib (Velcade; Millennium Pharmaceuticals, Cambridge, MA) was injected intravenously (1.3 mg/m^2 body surface area) on *days 1*, *4*, *8*, and *11*. Similar dose and scheme were previously used in a

phase 2 study of bortezomib for the treatment of multiple myeloma (40). Control animals were injected on the same days with an equal volume (0.6 ml) of the vehicle saline (0.9%). One hour after the last injection, animals were killed as described above.

Measurement of proteasome activity

Proteasome activity was determined as described previously (33, 52). 20S proteasomes were isolated from solubilized diaphragm samples in ice-cold buffer (pH 7.5) containing 50 mM Tris·HCl, 5 mM $MgCl_2$, 250 mM sucrose, 1 mM 1,4-dithiothreitol, 0.2 mM phenylmethylsulfonyl fluoride, and protease inhibitor cocktail (Sigma Aldrich, Zwijndrecht, The Netherlands). After three sequential centrifugation steps of the supernatants at 10,000 *g* (20 min), 100,000 *g* (1 h), and 100,000 *g* (5 h), the final pellet was resuspended in buffer (pH 7.5) containing 50 mM Tris·HCl, 5 mM $MgCl_2$, and 20% glycerol. The protein content of the proteasome preparation was determined based on Bio-Rad Protein Assay (Bio-Rad, Veenendaal, The Netherlands). The proteolytic activity of the 20S proteasome extracts (15 μg) was determined by measuring the activity against the fluorogenic substrates succinyl-leu-leu-val-tyr-7-AMC (LLVY-AMC) (Sigma-Aldrich). The peptidase activity was determined by measuring the generation of the fluorogenic cleavage product (AMC) at 355 nM excitation wavelength and 460 nM emission wavelength. AMC standards were used to quantify activity levels. Addition of a specific proteasome inhibitor (MG-132) confirmed specificity of the assay.

Diaphragm muscle single fiber contractile measurements

Single fiber contractile measurements and experimental protocol were performed according to previously described methods (52). In short, a rectangular bundle from the central costal region of the right hemidi-aphragm was dissected, parallel to the long axis of the muscle fibers. The muscle bundle was transferred to relaxing solution (5°C) containing 1% Triton X-100 to permeabilize lipid membranes. Subsequently, single fibers were isolated from the muscle bundle, attached to aluminum foil clips, and mounted in a temperature-controlled (20°C) flow-through acrylic chamber (120-μl volume) on two hooks connected to a force transducer (model AE-801; SensoNor, Horten, Norway) and a servomotor (model 308B, Aurora Scientific). Sarcomere length was set at 2.4 μm as the optimal length for force generation. Muscle fiber cross-sectional area was deduced from fiber width and depth measurements using a reticule in the microscope eyepiece. MIDAC software (Radboud Univ. Nijmegen, The Netherlands) and a data acquisition board were used to record signals. Maximum isometric force was determined by measuring force after perfusing the experimental chamber with, successively, pCa 9.0 and pCa 4.0 solutions. Maximum specific force was derived from dividing maximum isometric force by fiber cross-sectional area. The rate constant for tension redevelopment (k_{tr}) was measured as described by Brenner and Eisenberg (8) during activation at pCa 4.0. In short, fibers were rapidly released by ~15%, and then ~50 ms later, restretched to their original length. During the rapid release and restretch, cross-bridges detach, and force drops to zero. The cross-bridges then reattach, and force redevelops. As published previously (19), the k_{tr} value was determined using a computer algorithm for least-squares fit of a first-order exponential.

Myosin heavy chain isoform composition and content per half sarcomere determination

Determination of myosin heavy chain iso-form composition and content by SDS-PAGE was described previously (52) and adapted from Geiger et al. (17). In short, single fibers were detached from the force transducer and servo-motor and solubilized in 25 μl of SDS sample buffer. Sample volumes of 8 μl were loaded on 7% SDS-polyacrylamide gels to separate proteins. Gels were silver stained according to the procedure described by Oakley et al. (32). Myosin heavy chain isoforms were identified by comparing migration patterns with those of control rat diaphragm bundle samples run on the same gels. After densitometer imaging

(Syngene, Cambridge, UK), myosin heavy chain content in the muscle fibers was deduced from the optical densities of known contents of purified rabbit myosin heavy chain (Sigma Aldrich) run on every gel. Myosin heavy chain content per half sarcomere, at sarcomere length of 2.4 μm, was calculated through dividing fiber myosin heavy chain content by the number of half-sarcomeres (2× length of fiber/2.4).

Western blots

For determining the proteasome content, diaphragm samples were homogenized in ~200 μl of ice-cold buffer (pH 7.5) containing 50 mM Tris, 1 mM EDTA, 1 mM dithiothreitol, 1 mM phenylmethylsulfonyl fluoride, and protease inhibitor cocktail (Sigma Aldrich). Homogenates were centrifuged at 10,000 *g* at 4°C for 10 min. For determining the amount of ubiquitinated myosin and total myosin, diaphragm samples were homogenized in 100 volumes of ice-cold buffer, pH 7.4 (20 mM Tris, 20 mM EGTA, 1 mM DTT, protease inhibitor cocktail, 0.5% SDS), boiled for 1 min, and centrifuged at 13,000 *g* at 20°C for 5 min. After protein concentration determination of the resulting supernatants, soluble proteins were subjected to routine Western blotting using polyacrylamide SDS-gels and specific antibodies (anti-20S proteasome subunit C8, Affiniti, Gorinchem, The Netherlands; anti-poly-ubiquitin, Biomol, Exeter, UK; anti-myosin heavy chain, Upstate Millipore, Amsterdam, The Netherlands). After washing, blots were incubated with a horseradish peroxidase-conjugated goat anti-mouse antibody (Pierce, Ettenleur, The Netherlands) for subsequent chemiluminescent detection. Protein bands were quantified using optical densitometry software (GeneTools, Syngene, UK).

MuRF-1 and MAFbx mRNA determination with real-time quantitative PCR

MuRF-1 and atrogin/MAFbx mRNA were determined as described previously (26, 33). Total RNA was extracted from diaphragm samples using TRIzol reagent (Invitrogen, Carlsbad, CA) and dissolved in diethylpyrocarbonate-treated water. Total RNA was reverse transcribed into cDNA using 50 ng of total RNA in a 20-μl reaction volume by using SuperScript Reverse Transcriptase (Invitrogen). Quantitative PCR was performed in a total reaction volume of 25 μl per reaction containing 12.5 μl of a SYBR green mix (Bio-Rad), 10 pmol of each forward and reverse primer, 1 μl cDNA, and nuclease-free water. Specific primer sets for rat MAFbx, MuRF-1, and glyceraldehyde-3-phosphate dehydrogenase (GAPDH) were purchased from SuperArray (Frederick, MD). PCR runs were performed in triplicate using MyiQ real-time PCR detection system (Bio-Rad, Salt Lake City, UT). Levels of MAFbx and MuRF-1 mRNA were normalized to that of GAPDH in arbitrary units.

Measurement of caspase-3 activity

Caspase-3 activity was determined as described previously (33, 52). Frozen diaphragm samples were homogenized in a buffer containing 100 mM HEPES (pH 7.5), 10% sucrose, 0.1% Nonidet P-40, 10 mM dithiothreitol, and protease inhibitor cocktail (Sigma Aldrich). Homogenates were subjected to three cycles of freeze-thaw before centrifugation at 18,000 *g* for 30 min, and the supernatant (92.5 μg) was added to reaction buffer consisting of 100 mM HEPES (pH 7.5), 10% sucrose, and 10 mM dithiothreitol. The fluorogenic substrate *N*-acetyl-Asp-Glu-Val-Asp-7-amido-4-methylcoumarin (Ac-DEVD-AMC) was then added, and the reaction was performed at 30°C for 60 min. The caspase-3 activity was determined by measuring the generation of the fluorogenic cleavage product methylcoumarylamide (AMC) from the fluorogenic substrate Ac-DEVD-AMC at 360 nM excitation wavelength and 460 nM emission wavelength. AMC standards were used to quantify activity levels. Specificity of the assay was confirmed by addition of the specific caspase-3 inhibitor Ac-DEVD-CHO to the reaction mixture.

Data treatment and statistical methods

All data represent the mean ± SE of at least six animals in each group. Single fiber data were grouped per fiber types slow and 2x and averaged per rat, with two to four fibers measured per rat. Differences between groups were analyzed with a one-way ANOVA. Student-Newman-Keuls post hoc testing was performed on data from CHF saline vs. CHF bortezomib groups and sham saline vs. sham bortezomib groups. Because of a limited amount of diaphragm tissue per rat, proteasome activity, caspase-3 activity, MuRF-1 and MAFbx mRNA levels, and Western blotting studies are not based on the same animals, although there is extensive overlap. A probability level of $P < 0.05$ was considered significant unless otherwise indicated.

RESULTS

CHF indexes

As previously reported (52), CHF was characterized by reduced systolic and elevated diastolic left ventricular pressures, pulmonary congestion, and cardiomegaly (see Table 1). Bortezomib treatment did not significantly affect body weight and the severity of heart failure, as indicated by similar blood pressures, heart weights, infarct sizes, and lung weight wet-to-dry ratios in CHF rats treated with bortezomib and saline.

Proteasome activity

20S proteasome activity was higher in the diaphragm from CHF-saline rats than sham-saline ($P < 0.05$), and bortezomib treatment significantly inhibited proteasome activity in both CHF and sham rats (Fig. 1*A*). To investigate if changes in proteasome activity are the result of changes in the number of proteasomes, we determined the protein level of the C8 subunit of the 20S proteasome. Figure 1*B* demonstrates that CHF and bortezomib treatment did not significantly affect proteasome content in the diaphragm.

Diaphragm muscle single fiber contractility

In line with our previous findings (52), CHF decreased maximal force generation in rat diaphragm single fibers ($P < 0.01$, Fig. 2*A*). Bortezomib treatment increased maximal force generation in diaphragm fibers from CHF rats ($P < 0.05$). The k_{tr} was used as a measure for cross-bridge cycling kinetics. K_{tr} was lower in diaphragm fibers from CHF saline rats than sham ($P < 0.01$, Fig. 2*B*). Bortezomib treatment improved k_{tr} in CHF diaphragm fibers ($P < 0.01$). In sham, however, no effect of bortezomib treatment on maximal force generation and k_{tr} was observed. These findings were observed in two most predominant rat diaphragm fiber types, slow and 2x.

Diaphragm single fiber myosin content

Myosin content per half sarcomere was reduced in diaphragm fibers from CHF-saline rats compared with sham-saline ($P < 0.05$, Fig. 3*A*). Bortezomib treatment increased myosin content per half sarcomere in CHF diaphragm fibers of both type slow and 2x ($P < 0.05$). In sham, bortezomib did not alter myosin content per half sarcomere. Cross-sectional area of diaphragm fibers were not significantly affected by CHF or bortezomib treatment (Fig. 3*B*). Alterations in maximal force generating capacity were proportional to changes in myosin content per half sarcomere (Fig. 3*C*).

Ubiquitinated myosin levels

Ubiquitinated myosin heavy chain levels were determined by Western blotting. Because total myosin content of the diaphragm is affected by both CHF and proteasome inhibition (Fig. 3), the amount of ubiquitinated myosin was normalized for total myosin content.

Myosin ubiquitination was higher in diaphragm homogenates from CHF rats compared with sham ($P < 0.05$, Fig. 4). Bortezomib treatment increased levels of ubiquitinated myosin in sham ($P < 0.05$), but not significantly ($P = 0.17$) in CHF.

MuRF-1 and MAFbx mRNA

Compared to sham-saline, mRNA levels of MuRF-1 and MAFbx were higher in the diaphragm muscle of CHF-saline rats ($P < 0.01$, Fig. 5). Bortezomib treatment resulted in a downregulation of MuRF1 and MAFbx mRNA expression in CHF (respectively, $P < 0.05$ and $P = 0.06$), but not in sham.

Caspase-3 activity

Caspase-3 activity was higher in diaphragm homogenates from CHF-saline rats than sham-saline ($P < 0.05$; Fig. 6*A*). Bortezomib treatment significantly decreased caspase-3 activity in the diaphragm of CHF and sham rats.

Inhibition of caspase-3 by bortezomib was an unexpected finding. To examine if bortezomib directly inhibits caspase-3, we measured cleaving activity of recombinant caspase-3 in the presence and absence of 25 nM bortezomib in vitro. Bortezomib did not affect recombinant caspase-3 activity (Fig. 6*B*). However, addition of bortezomib to diaphragm homogenates of untreated CHF and sham rats decreased caspase-3 activity. This indicates that bortezomib inhibited caspase-3 in an indirect fashion.

DISCUSSION

This study is the first to show that modulation of proteasome activity improves diaphragm contractility in an animal model associated with muscle wasting. Treatment with the proteasome inhibitor bortezomib increased diaphragm contractility in CHF rats by restoring myosin content. In addition, our data show that proteasome inhibition affects mediators upstream of the proteasome, like MuRF-1 and caspase-3. These findings improve the understanding of respiratory muscle wasting in CHF and provide a rationale for investigating the therapeutic applicability of modulating ubiquitin-proteasome activation in muscle wasting conditions.

Myosin degradation by the proteasome in CHF diaphragm

Recently, treatment with bortezomib has been shown to prevent muscle weight loss in experimental muscle wasting (4, 23, 24). In the present study, we used a clinical dosage of bortezomib to investigate the effect of proteasome inhibition on recovery of specific contractile protein loss and muscle dysfunction. The contractile protein myosin seems to be selectively targeted by the ubiquitin-proteasome pathway during peripheral muscle wasting in cancer cachexia (1). In accordance with those observations, our data provide additional evidence for proteasome-dependent myosin degradation, as in vivo proteasome inhibition increased myosin content in the CHF diaphragm muscle.

Of special interest is our finding that restoring myosin content by proteasome inhibition partially reverses diaphragm muscle weakness in CHF animals. This implicates that diaphragm weakness results from increased myosin degradation by the proteasome. Furthermore, the rise in maximal force generation is proportional to the rise in myosin content in CHF diaphragm fibers (Fig. 3*C*). Thus maximal force per myosin content was not affected by bortezomib treatment in CHF. When one presumes that bortezomib does not affect the trigger for respiratory muscle wasting, at least bortezomib did not change the severity of CHF (Table 1), then these data indicate that the proteasome degrades myosin that is not functionally compromised. Indeed, the ubiquitin-proteasome pathway plays a key role

in recognition and subsequent degradation of dysfunctional proteins, but is involved in the turnover of functional proteins as well (25, 39). Therefore, it seems that diaphragm dysfunction in CHF results from a general imbalance between protein degradation and synthesis, rather than from an increased degradation of dysfunctional proteins. The effects of proteasome inhibition on protein synthesis have not been studied yet.

Interestingly, bortezomib treatment not only improved maximal force generation of CHF diaphragm fibers, but increased the rate constant of tension redevelopment as well. The rate constant of tension redevelopment is an estimate for cross-bridge cycling kinetics (44), which are slowed in CHF diaphragm (10, 52). Impaired cross-bridge cycling kinetics may arise from increased oxidation of contractile proteins (19, 35, 36, 41), but could also be a result of increased myofilament lattice spacing (30, 45). Although we cannot exclude that proteasome inhibition affects contractile protein oxidation, our data support the involvement of increased myofilament lattice spacing in CHF diaphragm dysfunction, as proteasome inhibition restored myosin concentration and improved the rate constant of tension redevelopment.

In the present study, proteasome inhibition in CHF was effective, but did not completely restore diaphragm function. Bortezomib incompletely inhibited proteasome activities (Fig. 1), but it is unlikely that a complete proteasome inhibition would fully restore diaphragm function. On the contrary, given the fact that the ubiquitin-proteasome pathway serves basic housekeeping cell functions, the incomplete inhibition may suggest a therapeutic window between beneficial and toxic effects. A more likely explanation for incomplete recovery of diaphragm function is the relative short duration of treatment with respect to the chronic stage of disease. In addition, although the present study demonstrates major accountability for the ubiquitin-proteasome pathway in effectuating diaphragm dysfunction, we cannot exclude the possible involvement of proteasome-independent pathways. For example, increased lysosomal degradation and calpain activities have also been associated with diaphragm wasting (28). In contrast to other proteasome inhibitors, like MG-132 and lactacystin, bortezomib is highly specific for the proteasome and does not target these proteolytic systems (22). Thus, the recovery of diaphragm function in the present study is most likely to be the result of proteasome inhibition.

Proteasome inhibition in healthy diaphragm

The present study clearly shows that treatment with a highly specific proteasome inhibitor improves diaphragm function by restoring myosin content in CHF. Although not the main focus of this study, we also determined the effect of bortezomib on diaphragm function in healthy animals. Interestingly, proteasome inhibition did not affect diaphragm function and myosin content in healthy animals. As myosin is the most predominant muscle protein, this observation is in line with previously reported unaltered muscle weight of healthy animals treated with bortezomib (4, 23). Thus, treatment with a highly specific proteasome inhibitor restores myosin content in pathological conditions, but proteasome inhibition seems not to be sufficient to induce muscle growth, i.e., hypertrophy. Unaltered cross-sectional areas of fibers from bortezomib-treated rats, both CHF and healthy, confirm the absence of fiber hypertrophy (Fig. 3*B*). Therefore, our results strongly suggest that recovery of myosin loss and hypertrophy follow different mechanisms.

Proteasome inhibition and upstream signaling pathways

Most proteins to be degraded by the proteasome are in advance marked for degradation by covalent linkage to a chain of ubiquitin (18, 47). Proteasome inhibition has previously been demonstrated to result in accumulation of ubiquitinated proteins (50). Indeed, in the present study, bortezomib treatment increased the levels of ubiquitinated myosin in sham-operated

rats. Unexpectedly, proteasome inhibition by bortezomib did not significantly increase ubiquitinated myosin levels in CHF rats (Fig. 4), indicating reduced myosin ubiquitination. MuRF-1 plays a prominent role in ubiquitination of myosin (9, 14). In line with these observations, in our study, bortezomib reduced MuRF-1 expression in CHF diaphragm, but not in sham (Fig. 5), providing an explanation for the absence of raised ubiquitinated myosin levels after bortezomib treatment in CHF (Fig. 4). Indeed, reduced expression of E3-ligases after bortezomib treatment has been reported previously in burn-induced muscle atrophy (24). The mechanism of bortezomib-induced reduction in MuRF-1 expression has not been studied.

Regulation of caspase-3 by bortezomib

For improved muscle function, myosin should not only be intact and functional, but as well have retained its position in the sarcomere. Caspase-3 is one of the proteolytic enzymes that is thought to cleave myofilaments from the sarcomere preceding degradation by the proteasome (13). Previous studies demonstrated that caspase-3 is activated during muscle wasting (5, 33, 48, 52). The present study shows that bortezomib treatment decreased caspase-3 activity in the diaphragm muscle of CHF rats. This could be a critical step in prevention of CHF-induced atrophy. Furthermore, caspase-3 inhibition could play a role in diminishing MuRF-1 and MAFbx levels, as administration of a caspase-3 inhibitor in muscle-wasted mice decreased mRNA expression of these E3-ligases (48). Thus, the effects of bortezomib on myosin content and diaphragm function might be mediated by reducing caspase-3 activity.

Our finding that bortezomib treatment decreases caspase-3 activity in the diaphragm muscle is surprising, as several studies have shown that bortezomib induces apoptosis by activating caspase-3 in cancer cell lines (16, 20, 38, 43). Previously, it has been postulated that the effect of proteasome inhibition on caspase-3 depends on cell cycle status (12), as proteasome inhibition induces apoptosis in proliferating cells, while it protects terminally differentiated cells from apoptosis. The muscle fiber is terminally differentiated, thus our findings are consistent with the cell cycle dependency of proteasome inhibition on caspase-3 activity. Importantly, bortezomib in vitro does not affect recombinant caspase-3 (Fig. 6*B*), providing evidence for indirect inhibition of caspase-3 by bortezomib. For example, decreased proteasomal degradation of caspase-3 inhibitor XIAP may play a role (46). Furthermore, a recent study demonstrated that bortezomib increased levels of caspase-8 inhibitor c-FLIP (27), and caspase-8 has been shown to be responsible for caspase-3 activation in an inflammation model for diaphragm weakness (49). Thus, it seems that subsequent effects of proteasome inhibition, i.e., caspase-3 inhibition, are involved in effectuating the recovery of diaphragm function in CHF rats. However, future studies with specific caspase-3 inhibitors are needed to establish the exact role of caspase-3 activation in CHF diaphragm dysfunction.

Bortezomib

Bortezomib is the first proteasome inhibitor approved for use in humans and used for treatment of multiple myeloma (40). Bortezomib is a monomeric boronic acid that interacts with a threonine residue located on the β-subunit that confers chymotryptic-like proteolytic activity of the 26S proteasome (2). Peptide boronic acids, such as bortezomib, are highly specific and up to 100-fold more potent than their peptide aldehyde analogs (3). Together with its relatively mild toxicity (40), this makes bortezomib the best drug candidate to study the proteasome dependency of muscle weakness in vivo. The present data show that bortezomib treatment (intravenously) in CHF rats reduces proteasome activity in the diaphragm muscle. Although a tendency towards decreased proteasome content in bortezomib-treated animals was observed, differences between groups did not reach

statistical significance (Fig. 1*B*). This indicates that bortezomib primarily inhibits proteolytic activity per proteasome.

In conclusion, the present study demonstrates that in vivo treatment with a proteasome inhibitor improves diaphragm contractility by restoring myosin content in CHF. Proteasome inhibition may exert these positive effects by subsequently affecting caspase-3 and muscle-specific E3-ligases. Despite its availability for human use, the application of bortezomib in CHF is at this moment strictly experimental. Investigating the effectiveness of bortezomib in other models for muscle wasting, such as COPD (33), mechanical ventilation (42), sepsis (15), and cancer (51) is needed to further explore the therapeutic applicability of modulating ubiquitin-proteasome activation to recover contractile function in muscle weakness.

Acknowledgments

We thank the group of Dr. Decramer and Dr. Gayan-Ramirez from the University of Leuven, Belgium, for assistance in the development of the CHF rat model and Leo Ennen, Central Animal Laboratory in Nijmegen, The Netherlands, for performing the coronary artery ligations.

GRANTS

This study was funded by an unrestricted educational grant from Novartis, The Netherlands. A part of the presented work was supported by National Institute of Arthritis and Musculoskeletal and Skin Diseases Grant AR-052511 (to Y.-P. Li).

References

1. Acharyya S, Ladner KJ, Nelsen LL, Damrauer J, Reiser PJ, Swoap S, Guttridge DC. Cancer cachexia is regulated by selective targeting of skeletal muscle gene products. J Clin Invest. 2004; 114:370–378. [PubMed: 15286803]
2. Adams J. The proteasome: structure, function, and role in the cell. Cancer Treat Rev. 2003; 29(Suppl 1):3–9. [PubMed: 12738238]
3. Adams J, Behnke M, Chen S, Cruickshank AA, Dick LR, Grenier L, Klunder JM, Ma YT, Plamondon L, Stein RL. Potent and selective inhibitors of the proteasome: dipeptidyl boronic acids. Bioorg Med Chem Lett. 1998; 8:333–338. [PubMed: 9871680]
4. Beehler BC, Sleph PG, Benmassaoud L, Grover GJ. Reduction of skeletal muscle atrophy by a proteasome inhibitor in a rat model of denervation. Exp Biol Med. 2006; 231:335–341.
5. Belizario JE, Lorite MJ, Tisdale MJ. Cleavage of caspases-1, -3, -6, -8 and -9 substrates by proteases in skeletal muscles from mice undergoing cancer cachexia. Br J Cancer. 2001; 84:1135–1140. [PubMed: 11308266]
6. Bodine SC, Latres E, Baumhueter S, Lai VK, Nunez L, Clarke BA, Poueymirou WT, Panaro FJ, Na E, Dharmarajan K, Pan ZQ, Valenzuela DM, DeChiara TM, Stitt TN, Yancopoulos GD, Glass DJ. Identification of ubiquitin ligases required for skeletal muscle atrophy. Science. 2001; 294:1704–1708. [PubMed: 11679633]
7. Brenner B. Effect of Ca^{2+} on cross-bridge turnover kinetics in skinned single rabbit psoas fibers: implications for regulation of muscle contraction. Proc Natl Acad Sci USA. 1988; 85:3265–3269. [PubMed: 2966401]
8. Brenner B, Eisenberg E. Rate of force generation in muscle: correlation with actomyosin ATPase activity in solution. Proc Natl Acad Sci USA. 1986; 83:3542–3546. [PubMed: 2939452]
9. Clarke BA, Drujan D, Willis MS, Murphy LO, Corpina RA, Burova E, Rakhilin SV, Stitt TN, Patterson C, Latres E, Glass DJ. The E3 ligase MuRF1 degrades myosin heavy chain protein in dexamethasone-treated skeletal muscle. Cell Metab. 2007; 6:376–385. [PubMed: 17983583]
10. Coirault C, Guellich A, Barbry T, Samuel JL, Riou B, Lecarpentier Y. Oxidative stress of myosin contributes to skeletal muscle dysfunction in rats with chronic heart failure. Am J Physiol Heart Circ Physiol. 2007; 292:H1010–H1017.

11. Dewys WD, Begg C, Lavin PT, Band PR, Bennett JM, Bertino JR, Cohen MH, Douglass HO Jr, Engstrom PF, Ezdinli EZ, Horton J, Johnson GJ, Moertel CG, Oken MM, Perlia C, Rosenbaum C, Silver-stein MN, Skeel RT, Sponzo RW, Tormey DC. Prognostic effect of weight loss prior to chemotherapy in cancer patients. Eastern Cooperative Oncology Group. Am J Med. 1980; 69:491–497. [PubMed: 7424938]
12. Drexler HC. Activation of the cell death program by inhibition of proteasome function. Proc Natl Acad Sci USA. 1997; 94:855–860. [PubMed: 9023346]
13. Du J, Wang X, Miereles C, Bailey JL, Debigare R, Zheng B, Price SR, Mitch WE. Activation of caspase-3 is an initial step triggering accelerated muscle proteolysis in catabolic conditions. J Clin Invest. 2004; 113:115–123. [PubMed: 14702115]
14. Fielitz J, Kim MS, Shelton JM, Latif S, Spencer JA, Glass DJ, Richardson JA, Bassel-Duby R, Olson EN. Myosin accumulation and striated muscle myopathy result from the loss of muscle RING finger 1 and 3. J Clin Invest. 2007; 117:2486–2495. [PubMed: 17786241]
15. Friedrich O. Critical illness myopathy: what is happening? Curr Opin Clin Nutr Metab Care. 2006; 9:403–409. [PubMed: 16778569]
16. Gatto S, Scappini B, Pham L, Onida F, Milella M, Ball G, Ricci C, Divoky V, Verstovsek S, Kantarjian HM, Keating MJ, Cortes-Franco JE, Beran M. The proteasome inhibitor PS-341 inhibits growth and induces apoptosis in Bcr/Abl-positive cell lines sensitive and resistant to imatinib mesylate. Haematologica. 2003; 88:853–863. [PubMed: 12935973]
17. Geiger PC, Cody MJ, Macken RL, Sieck GC. Maximum specific force depends on myosin heavy chain content in rat diaphragm muscle fibers. J Appl Physiol. 2000; 89:695–703. [PubMed: 10926656]
18. Hershko A, Ciechanover A, Heller H, Haas AL, Rose IA. Proposed role of ATP in protein breakdown: conjugation of protein with multiple chains of the polypeptide of ATP-dependent proteolysis. Proc Natl Acad Sci USA. 1980; 77:1783–1786. [PubMed: 6990414]
19. Heunks LM, Cody MJ, Geiger PC, Dekhuijzen PN, Sieck GC. Nitric oxide impairs Ca^{2+} activation and slows cross-bridge cycling kinetics in skeletal muscle. J Appl Physiol. 2001; 91:2233–2239. [PubMed: 11641366]
20. Hideshima T, Richardson P, Chauhan D, Palombella VJ, Elliott PJ, Adams J, Anderson KC. The proteasome inhibitor PS-341 inhibits growth, induces apoptosis, and overcomes drug resistance in human multiple myeloma cells. Cancer Res. 2001; 61:3071–3076. [PubMed: 11306489]
21. Hughes PD, Polkey MI, Harrus ML, Coats AJ, Moxham J, Green M. Diaphragm strength in chronic heart failure. Am J Respir Crit Care Med. 1999; 160:529–534. [PubMed: 10430724]
22. Kisselev AF, Goldberg AL. Proteasome inhibitors: from research tools to drug candidates. Chem Biol. 2001; 8:739–758. [PubMed: 11514224]
23. Krawiec BJ, Frost RA, Vary TC, Jefferson LS, Lang CH. Hindlimb casting decreases muscle mass in part by proteasome-dependent proteolysis but independent of protein synthesis. Am J Physiol Endocrinol Metab. 2005; 289:E969–E980. [PubMed: 16046454]
24. Lang CH, Huber D, Frost RA. Burn-induced increase in atrogin-1 and MuRF-1 in skeletal muscle is glucocorticoid independent but downregulated by IGF-I. Am J Physiol Regul Integr Comp Physiol. 2007; 292:R328–R336. [PubMed: 16946078]
25. Lecker SH, Goldberg AL, Mitch WE. Protein degradation by the ubiquitin-proteasome pathway in normal and disease states. J Am Soc Nephrol. 2006; 17:1807–1819. [PubMed: 16738015]
26. Li YP, Chen Y, John J, Moylan J, Jin B, Mann DL, Reid MB. TNF-alpha acts via p38 MAPK to stimulate expression of the ubiquitin ligase atrogin1/MAFbx in skeletal muscle. FASEB J. 2005; 19:362–370. [PubMed: 15746179]
27. Liu X, Yue P, Chen S, Hu L, Lonial S, Khuri FR, Sun SY. The proteasome inhibitor PS-341 (bortezomib) up-regulates DR5 expression leading to induction of apoptosis and enhancement of TRAIL-induced apoptosis despite up-regulation of c-FLIP and survivin expression in human NSCLC cells. Cancer Res. 2007; 67:4981–4988. [PubMed: 17510429]
28. Maes K, Testelmans D, Powers S, Decramer M, Gayan-Ramirez G. Leupeptin inhibits ventilator-induced diaphragm dysfunction in rats. Am J Respir Crit Care Med. 2007; 175:1134–1138. [PubMed: 17379854]

29. Mancini DM, Henson D, LaManca J, Levine S. Respiratory muscle function and dyspnea in patients with chronic congestive heart failure. Circulation. 1992; 86:909–918. [PubMed: 1516204]
30. McDonald KS, Wolff MR, Moss RL. Sarcomere length dependence of the rate of tension redevelopment and submaximal tension in rat and rabbit skinned skeletal muscle fibres. J Physiol. 1997; 501:607–621. [PubMed: 9218220]
31. Meyer FJ, Borst MM, Zugck C, Kirschke A, Schellberg D, Kubler W, Haass M. Respiratory muscle dysfunction in congestive heart failure: clinical correlation and prognostic significance. Circulation. 2001; 103:2153–2158. [PubMed: 11331255]
32. Oakley BR, Kirsch DR, Morris NR. A simplified ultrasensitive silver stain for detecting proteins in polyacrylamide gels. Anal Biochem. 1980; 105:361–363. [PubMed: 6161559]
33. Ottenheijm CA, Heunks LM, Li YP, Jin B, Minnaard R, van Hees HW, Dekhuijzen PN. Activation of the ubiquitin-proteasome pathway in the diaphragm in chronic obstructive pulmonary disease. Am J Respir Crit Care Med. 2006; 174:997–1002. [PubMed: 16917114]
34. Ottenheijm CA, Heunks LM, Sieck GC, Zhan WZ, Jansen SM, Degens H, de Boo T, Dekhuijzen PN. Diaphragm dysfunction in chronic obstructive pulmonary disease. Am J Respir Crit Care Med. 2005; 172:200–205. [PubMed: 15849324]
35. Park HS, Gong BJ, Tao T. A disulfide crosslink between Cys98 of troponin-C and Cys133 of troponin-I abolishes the activity of rabbit skeletal troponin. Biophys J. 1994; 66:2062–2065. [PubMed: 8075339]
36. Perkins WJ, Han YS, Sieck GC. Skeletal muscle force and actomyosin ATPase activity reduced by nitric oxide donor. J Appl Physiol. 1997; 83:1326–1332. [PubMed: 9338443]
37. Pfeffer MA, Pfeffer JM, Fishbein MC, Fletcher PJ, Spadaro J, Kloner RA, Braunwald E. Myocardial infarct size and ventricular function in rats. Circ Res. 1979; 44:503–512. [PubMed: 428047]
38. Pham LV, Tamayo AT, Yoshimura LC, Lo P, Ford RJ. Inhibition of constitutive NF-kappa B activation in mantle cell lymphoma B cells leads to induction of cell cycle arrest and apoptosis. J Immunol. 2003; 171:88–95. [PubMed: 12816986]
39. Reinstein E, Ciechanover A. Narrative review: protein degradation and human diseases: the ubiquitin connection. Ann Intern Med. 2006; 145:676–684. [PubMed: 17088581]
40. Richardson PG, Barlogie B, Berenson J, Singhal S, Jagannath S, Irwin D, Rajkumar SV, Srkalovic G, Alsina M, Alexanian R, Siegel D, Orlowski RZ, Kuter D, Limentani SA, Lee S, Hideshima T, Esseltine DL, Kauffman M, Adams J, Schenkein DP, Anderson KC. A phase 2 study of bortezomib in relapsed, refractory myeloma. N Engl J Med. 2003; 348:2609–2617. [PubMed: 12826635]
41. Root DD, Cheung P, Reisler E. Catalytic cooperativity induced by SH1 labeling of myosin filaments. Biochemistry. 1991; 30:286–294. [PubMed: 1824816]
42. Schweickert WD, Hall J. ICU-acquired weakness. Chest. 2007; 131:1541–1549. [PubMed: 17494803]
43. Shah SA, Potter MW, McDade TP, Ricciardi R, Perugini RA, Elliott PJ, Adams J, Callery MP. 26S proteasome inhibition induces apoptosis and limits growth of human pancreatic cancer. J Cell Biochem. 2001; 82:110–122. [PubMed: 11400168]
44. Sieck GC, Prakash YS. Cross-bridge kinetics in respiratory muscles. Eur Respir J. 1997; 10:2147–2158. [PubMed: 9311518]
45. Sieck GC, Zhan WZ, Han YS, Prakash YS. Effect of denervation on ATP consumption rate of diaphragm muscle fibers. J Appl Physiol. 2007; 103:858–866. [PubMed: 17556500]
46. Sohn D, Totzke G, Essmann F, Schulze-Osthoff K, Levkau B, Janicke RU. The proteasome is required for rapid initiation of death receptor-induced apoptosis. Mol Cell Biol. 2006; 26:1967–1978. [PubMed: 16479014]
47. Solomon V, Baracos V, Sarraf P, Goldberg AL. Rates of ubiquitin conjugation increase when muscles atrophy, largely through activation of the N-end rule pathway. Proc Natl Acad Sci USA. 1998; 95:12602–12607. [PubMed: 9770532]
48. Song YH, Li Y, Du J, Mitch WE, Rosenthal N, Delafontaine P. Muscle-specific expression of IGF-1 blocks angiotensin II-induced skeletal muscle wasting. J Clin Invest. 2005; 115:451–458. [PubMed: 15650772]

49. Supinski GS, Ji X, Wang W, Callahan LA. The extrinsic caspase pathway modulates endotoxin-induced diaphragm contractile dysfunction. J Appl Physiol. 2007; 102:1649–1657. [PubMed: 17218430]

50. Tawa NE Jr, Odessey R, Goldberg AL. Inhibitors of the proteasome reduce the accelerated proteolysis in atrophying rat skeletal muscles. J Clin Invest. 1997; 100:197–203. [PubMed: 9202072]

51. Tisdale MJ. Cachexia in cancer patients. Nat Rev Cancer. 2002; 2:862–871. [PubMed: 12415256]

52. van Hees HW, van der Heijden HF, Ottenheijm CA, Heunks LM, Pigmans CJ, Verheugt FW, Brouwer RM, Dekhuijzen PN. Diaphragm single-fiber weakness and loss of myosin in congestive heart failure rats. Am J Physiol Heart Circ Physiol. 2007; 293:H819–H828. [PubMed: 17449557]

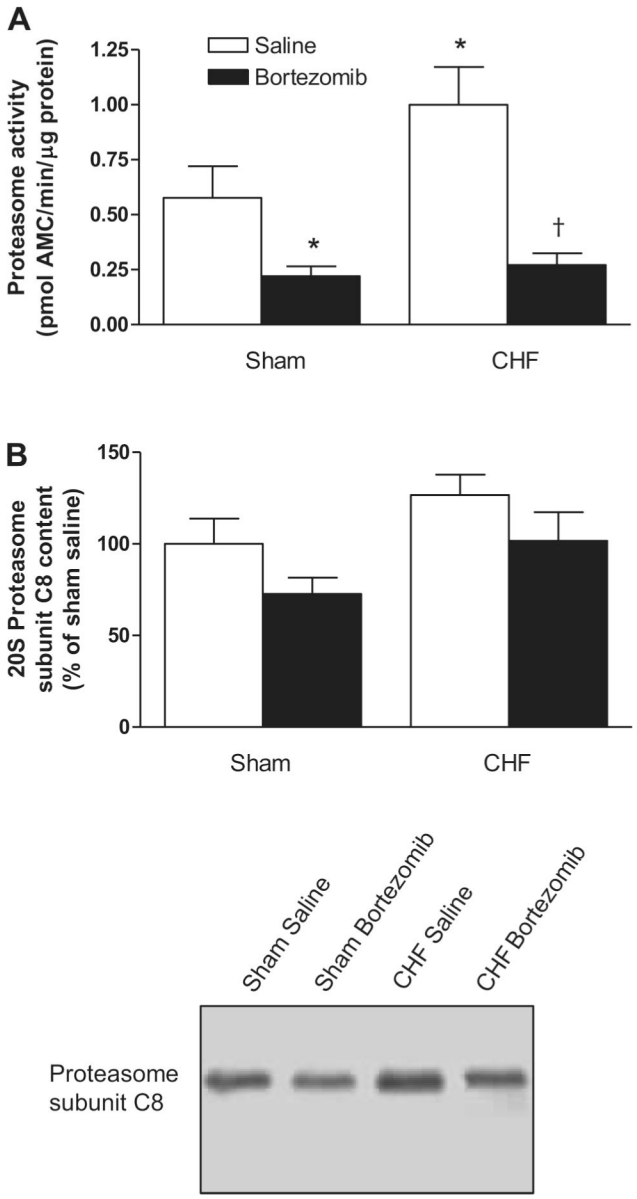

Fig. 1.

A: proteasome activity in diaphragm of congestive heart failure (CHF) and sham-operated rats treated with proteasome inhibitor bortezomib or saline (n = 6–7 per group). Proteasome activity was significantly higher in CHF saline diaphragm than in sham saline, and bortezomib treatment significantly reduced proteasome activity in the rat diaphragm. AMC, amido-4-methylcoumarin. Data are presented as means ± SE. *P < 0.05 vs. sham saline, †P < 0.01 vs. CHF saline. *B*: proteasome subunit C8 content as determined by Western blotting. *Top*: signals on blots were quantified with densitometry software. Bortezomib did not affect the amount of proteasomes in rat diaphragm. Data are presented as means ± SE. *Bottom*: representative immunoblots of proteasome subunit C8.

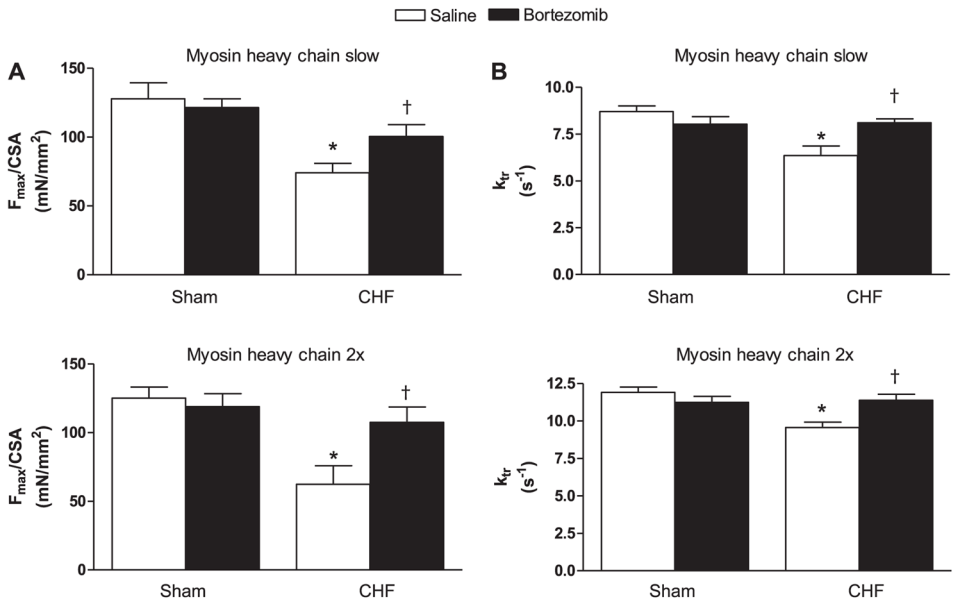

Fig. 2.

Diaphragm contractility in chemically skinned single fibers from CHF and sham-operated rats treated with proteasome inhibitor bortezomib or saline (n = 6–8 per group). Fibers are grouped per myosin heavy chain isoform slow and 2x. *A*: maximal force generation in diaphragm fibers from CHF saline rats was decreased compared with sham. Bortezomib treatment improved force generating capacity in CHF diaphragm fibers, but not in sham. CSA, cross-sectional area; F_{max}, maximal force at pCa 4.0. Data are presented as means ± SE. *P < 0.01 vs. sham saline, †P < 0.05 vs. CHF saline. *B*: the rate constant of force redevelopment (k_{tr}) was lower in diaphragm fibers from CHF saline rats compared with sham. Bortezomib treatment increased k_{tr} in CHF diaphragm fibers, but not in sham. Data are presented as means ± SE. *P < 0.01 vs. sham saline, †P < 0.01 vs. CHF saline.

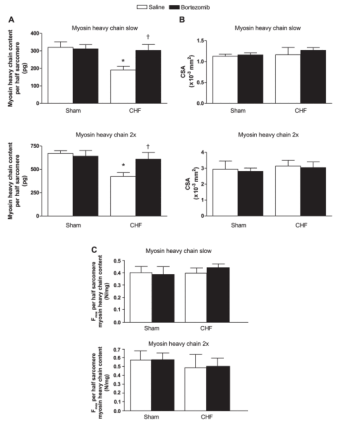

Fig. 3.

A: myosin heavy chain content per half sarcomere in diaphragm fibers from CHF and sham-operated rats treated with bortezomib or saline (n = 6–7 per group). Fibers are grouped per myosin heavy chain isoform slow and 2x. Myosin heavy chain content was lower in CHF saline diaphragm fibers than in sham. Bortezomib increased myosin heavy chain content in CHF diaphragm fibers, but not in sham. Data are presented as means ± SE. *P < 0.05 vs. sham saline, †P < 0.05 vs. CHF saline. *B*: cross-sectional areas of diaphragm fibers from CHF and sham-operated rats treated with bortezomib or saline (n = 6–7 per group). Fibers are grouped per myosin heavy chain isoform slow and 2x. CHF and bortezomib did not significantly affect cross-sectional fiber areas. Data are presented as means ± SE. *C*: maximal force (F_{max}) per half sarcomere myosin heavy chain content in diaphragm fibers from CHF and sham-operated rats treated with bortezomib or saline (n = 6–7 per group). Fibers are grouped per myosin heavy chain isoform slow and 2x. Neither CHF nor treatment with bortezomib significantly changed maximal force per half sarcomere myosin heavy chain content. Data are presented as means ± SE.

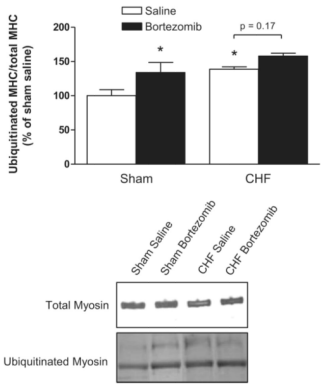

Fig. 4.

Ubiquitinated myosin levels in diaphragm from CHF and sham-operated rats treated with bortezomib or saline (n = 6–7 per group). *Top*: signals on blots were quantified with densitometry software. The amount of ubiquitinated myosin per total myosin in CHF diaphragm is higher than in sham. Ubiquitinated myosin levels increased in the diaphragm of bortezomib-treated rats compared with saline. *Bottom*: representative immunoblots of total myosin and ubiquitinated myosin. MHC, myosin heavy chain. Data are presented as means ± SE. *P < 0.05 vs. sham saline.

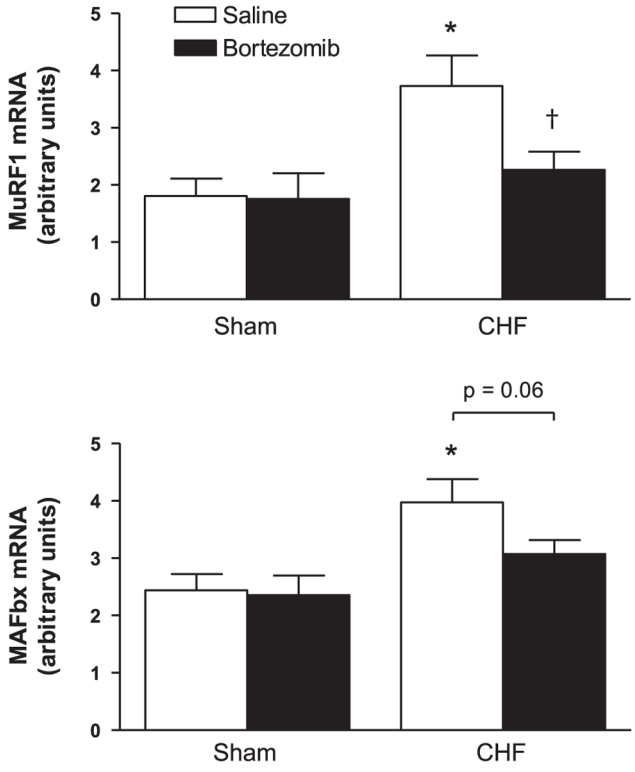

Fig. 5.

E3-ligase mRNA expression in diaphragm of CHF and sham-operated rats treated with bortezomib or saline (n = 7 per group). MuRF-1 and MAFbx mRNA expression are higher in CHF saline diaphragm than in sham saline. Bortezomib treatment results in a significant downregulation of MuRF-1 mRNA in CHF diaphragm. Data are presented as means ± SE. *P < 0.01 vs. sham saline, †P < 0.05 vs. CHF saline.

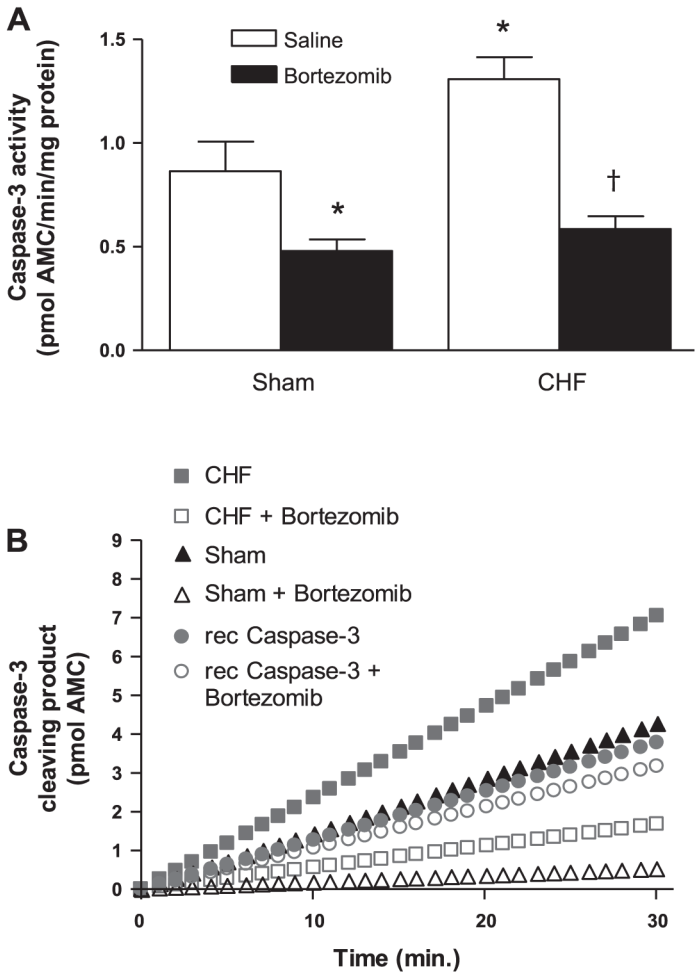

Fig. 6.

A: caspase-3 activity in diaphragm homogenates from CHF and sham-operated rats treated with bortezomib or saline (n = 6 per group). Caspase-3 activity was significantly higher in CHF saline diaphragm than in sham saline, and bortezomib treatment significantly reduced caspase-3 activity in the rat diaphragm. Data are presented as means ± SE. *$P < 0.05$ vs. sham saline, †$P < 0.01$ vs. CHF saline. *B*: the effect of bortezomib in vitro on caspase-3 activity. Diaphragm homogenates and recombinant caspase-3 (10 units) were subjected to caspase-3 activity assay in the presence and absence of (25 nM) bortezomib. Bortezomib in vitro did not affect recombinant caspase-3 cleaving rate, whereas bortezomib distinctly reduced caspase-3 cleaving rate of diaphragm homogenates from saline-treated sham rats and CHF rats.

Table 1

Animal characteristics of CHF and sham-operated rats treated with proteasome inhibitor bortezomib or saline

	Sham-Saline (*n* = 9)	Sham-Bortezomib (*n* = 8)	CHF-Saline (*n* = 13)	CHF-Bortezomib (*n* = 12)
BW (pretreatment), g	416±5	413±9	408±6	398±10
BW (end treatment), g	418±8	409±8	412±6	394±9
Aorta SP, mmHg	93±9	88±3	74±3*	74±2*
Aorta DP, mmHg	69±9	68±5	59±3	59±2
LV SP, mmHg	110±12	102±10	84±3*	77±3*
LV DP, mmHg	1±2	1±1	10±2*	11±3*
Heart weight, g	1.3±0.04	1.3±0.02	2.1±0.1*	2.1±0.1*
Infarct size, %			40±1	41±1
LW wet to dry ratio	4.5±0.1	4.5±0.1	4.9±0.1*	5.1±0.2*
LW/BW, mg/g	2.0±0.5	2.1±0.5	5.9±0.9*	6.1±1*

Data are presented as means ± SE.

*$P < 0.05$ vs. sham-saline.

BW, body weight; SP, systolic pressure; DP, diastolic pressure; LV, left ventricle; LW, lung weight.